Pure Appl. Geophys. 175 (2018), 3697–3718

https://doi.org/10.1007/s00024-018-1886-x

Pure and Applied Geophysics

Regional Climate Model Performance in Simulating Intra-seasonal and Interannual Variability of Indian Summer Monsoon

R. Bhatla,[1,2] Soumik Ghosh,[1] R. K. Mall,[2] P. Sinha,[3] and Abhijit Sarkar[4]

Abstract—Establishment of Indian summer monsoon (ISM) rainfall passes through the different phases and is not uniformly distributed over the Indian subcontinent. This enhancement and reduction in daily rainfall anomaly over the Indian core monsoon region during peak monsoon season (i.e., July and August) are commonly termed as 'active' and 'break' phases of monsoon. The purpose of this study is to analyze REGional Climate Model (RegCM) results obtained using the most suitable convective parameterization scheme (CPS) to determine active/break phases of ISM. The model-simulated daily outgoing longwave radiation (OLR), mean sea level pressure (MSLP), and the wind at 850 hPa of spatial resolution of 0.5°× 0.5° are compared with NOAA, NCEP, and EIN15 data, respectively over the South-Asia Co-Ordinated Regional Climate Downscaling EXperiment (CORDEX) region. 25 years (1986–2010) composites of OLR, MSLP, and the wind at 850 hPa are considered from start to the dates of active/break phase and up to the end dates of active/break spell of monsoon. A negative/positive anomaly of OLR with active/break phase is found in simulations with CPSs Emanuel and Mix99 (Grell over land; Emanuel over ocean) over the core monsoon region as well as over Monsoon Convergence Zone (MCZ) of India. The appearance of monsoon trough during active phase over the core monsoon zone and its shifting towards the Himalayan foothills during break phase are also depicted well. Because of multi-cloud function over oceanic region and single cloud function over the land mass, the Mix99 CPSs perform well in simulating the synoptic features during the phases of monsoon.

Key words: Active/break phase, Indian summer monsoon (ISM), REGional Climate Model (RegCM), CORDEX, convective parameterization scheme (CPS).

[1] Department of Geophysics, Institute of Science, Banaras Hindu University, Varanasi, India. E-mail: rbhatla@bhu.ac.in
[2] DST-Mahamana Centre of Excellence for Climate Change Research, Institute of Environment and Sustainable Development, Banaras Hindu University, Varanasi, India.
[3] School of Earth Ocean and Climate Sciences, Indian Institute of Technology (IIT), Bhubaneswar, India.
[4] National Centre for Medium Range Weather Forecasting (NCMRWF), Ministry of Earth Science, Noida, India.

Abbreviations

ISM	Indian summer monsoon
RegCM	REGional Climate Model by ICTP
CPS	Convective parameterization scheme
OLR	Outgoing longwave radiation
MSLP	Mean sea level pressure
NOAA	National Oceanic and Atmospheric Administration
NCEP	National Center for Environmental Prediction
EIN15	Era-Interim
MCZ	Monsoon Convergence Zone
CORDEX	Co-Ordinated Regional Climate Downscaling EXperiment
IMD	India Meteorological Department
IPCC	Intergovernmental panel on climate change
ICTP	International Center for Theoretical Physics
MM5	Mesoscale model version 5
BATS	Biosphere-atmosphere transfer scheme
PBL	Planetary boundary layer
ICBC	Initial conditions and boundary conditions
OISST	Optimum interpolation sea surface temperature
OI_WK	OISST in weekly pattern
NCC	National Climate Centre
Q–Q	Quantile–Quantile
SD	Standard deviation
RMSE	Root mean square error
CC	Correlation-coefficient
ECMWF	European Centre for Medium-Range Weather Forecasts
JJAS	June–July–August–September

1. Introduction

Southwest summer monsoon has an important role over Indian subcontinent which contributes about 80% of annual rainfall during June–September (JJAS). On the intra-seasonal time scale, the rainfall variability (enhancement and reduction) over the core monsoon region of India is demonstrated by "active" and "break" phases of monsoon. A small fluctuation in this intra-seasonal variability leads to the large-scale flood and drought over the Indian region. On the other hand, Indian total agriculture production highly depends on the seasonal rainfall and about 70% of working household strictly depends on agriculture activity as profession for livelihood (Krishna Kumar et al. 2004). Therefore, any inconsistency in intra-seasonal and intra-annual monsoon variability can have a major impact on Indian food grain production and India's economy can be badly affected by this variability (Gadgil et al. 1999; Krishna Kumar et al. 2004).

On Intra-seasonal time scale, the rainfall variability (enhancement and reduction) over the core monsoon zone of India is demonstrated by "active" and "break" phases of monsoon (Bhatla et al. 2004). In large-scale environment, these two regimes (active and break) are significantly different from the enhancement and depression of rainfall which depends on the northward propagation of convection from the central equatorial Indian Ocean to the Indian land region (Sikka and Gadgil 1980) and accompanied by eastward propagation of intra-seasonal events over the equatorial Indian Ocean (Lau and Chan 1986; Wang and Rui 1990; Lawrence and Webster 2002). Annamalai et al. (1999) have noted a northward propagation of convection zone which can often be associated with the start of active phases of rainfall (Krishnan et al. 2000; Lawrence and Webster 2002; Annamalai and Slingo 2001; Annamalai and Sperber 2005). A weak westward movement of convection toward the Indian continent has also been noted by Krishnamurti and Ardanuy (1980), Wang and Rui (1990), Annamalai and Slingo (2001). An opposite phenomenon in the active to break phase is consistent with the movement of monsoon trough which exists over India during the monsoon season (Ramamurthy 1969). He identified the minimum time span of the regular break period and very long break epochs that lasted for 17–20 days and occurs frequently during the peak monsoon months of July and August. Several studies based on different criteria over regions at differing spatial scales have been carried out to identify the active and break phases of ISM (Rajeevan et al. 2010; Krishnan et al. 2000; Annamalai and Slingo 2001). A comprehensive analysis using daily rainfall departures, wind anomalies and satellite-derived OLR which are associated with the commencement of the break monsoon condition has been studied by De and Mukhopadhyay (2002). The interrupted/continued rainfall distribution during ISM over the core monsoon zone is recognized as the most important feature of break/active (Gadgil 2003) and this particular climatic feature depends on various parameters. Therefore, various criteria have been adopted by IMD for defining the break condition over India (Rao 1976; Gadgil and Joseph 2003; Ramamurthy 1969; De et al. 1998). Rajeevan et al. (2010) have identified the break spells on the basis of gridded rainfall dataset depending on rainfall parameter only. The criteria of Krishnan et al. (2000) for identifying break condition completely depend on OLR composite analyses. They had conducted the spatial and temporal evaluations of convective anomalies associated with monsoon breaks with that of OLR-based diagnostic analyses. 17 years (1979–1995) of satellite-derived OLR and 850 hPa wind data from NCEP reanalysis were considered for their study. Their study demonstrated that the low latitude Rossby wave dynamics in the presence of a monsoon basic flow (which was driven by steady north–south differential heating) is the primary physical mechanism controlling monsoon active/breaks.

Several studies have been carried out to understand the intra-seasonal monsoon variability using climate modeling and simulation (Lal et al. 2000; Ajayamohan and Goswami 2007; Achuthavarier and Krishnamurthy 2009; Taraphdar et al. 2010; Goswami et al. 2012; Dash et al. 2014; Bhatla and Ghosh 2015). Many attempts have been made to evaluate the model with different CPSs to simulate ISM (Raju et al. 2015). The skill-based Regional Climate Model (RegCM) study has also been cried out by many scientists to simulate the intra-seasonal variability of monsoon (Bhate et al. 2012). Although, Kang and

Hong (2008) have specified that no specific scheme is entirely better than the others and in the modeling framework their performance varies with regions, simulated period, and interaction with other physical processes (IPCC 2007). Therefore, in recent decade, Giorgi et al. (2012) have introduced the updated version of RegCM-4 with the ability to run using different combinations of CPSs over land and ocean in mixed scheme mode. A limited efforts have been made to simulate ISM using RegCM over South-Asia CORDEX domain (Bhatla et al. 2016; Bhatla and Ghosh 2015; Raju et al. 2015; Maharana and Dimri 2015; Dash et al. 2014; Sinha et al. 2013). Moreover, simulation of monsoon using RegCM was found very sensitive with different cumulus parameterization schemes (Bhatla et al. 2016), particularly over the core monsoon region where convection plays a major role in monsoon dynamics (Dash et al. 2006; Sinha et al. 2013; Ghosh et al. 2018). It is also noticed that the performance of model always changes with the improved physics in the model (Umakanth et al. 2015).

Various studies have been carried out with the intra-seasonal variability of ISM using RegCM, but there are only few that cover the study of phases of ISM with the combination of CPSs over the specified region. In large-scale environment, the active and break regimes significantly influence the flood and the drought conditions over India. Therefore, this study is considered to analyze the active/break phases of ISM using RegCM-4.3 using combination of mixed scheme for simulation over core monsoon region and have tried to find out the best-suited CPSs of RegCM-4.3 in simulating active/break phases of monsoon. This work is in continuation of Bhatla et al. (2016), which focused on the onset phase simulation with the CPSs of RegCM-4.3. Their study has shown the performance of different CPSs over Indian land-sea continental margin during onset phase. Therefore, the primary objective of this study is to improve the current understanding of the intra-seasonal monsoon mechanism using different CPSs of RegCM-4.3 that controls the evaluation of active/breaks phases of monsoon. However, the model physics responsible for the intra-seasonal variability of ISM is not considered in this study.

2. *Model Description, Data and Experimental Design*

2.1. *Model Description*

The conceptual innovation of the RegCM-4.3 with the core of MM5 by ICTP was originally developed in late 1980s (Giorgi and Bates 1989; Dickinson et al. 1989). After a couple of major upgradation, Giorgi et al. (2012) have introduced 4.3 version of RegCM. In this version, two types of land-use have been added to BATS for the representation of urban and suburban environments. For urban development, surface albedo has been modified and surface energy balance is modified for altering the surface conditions. The physical processes of Holtslag et al. (1990) for the Planetary Boundary Layer (PBL) have been used for this study. RegCM-4.3 has four core CPSs; namely: Kuo, Tiedtke, Emanuel (Emanuel 1991; Emanuel and Živković-Rothman 1999) and Grell (Grell 1993). Besides, this version of RegCM-4.3 has the ability to run the combinations of different CPSs (Emanuel and Grell) separately over land and ocean in mixed convection schemes mode. The RegCM-4.3 configuration is placed in Table 1.

Table 1

Model configuration of RegCM-4.3

Dynamics	Hydrostatics
Model domain	South Asia CORDEX domain (15°S–45°N; 10°E–130°E)
Resolution	50 km horizontal
Vertical level	18 sigma vertical levels
Initial and boundary conditions	ERA15
SST	OI WK—OISST weekly optimal interpolation dataset
Land surface parameterization Radiation	Modified CCM3
Parameterization PBL	Modified holtslag
Convective parameterization	1. Mix98 (Emanuel over land and Grell over ocean) 2. Mix99 (Emanuel over ocean and Grell over land) 3. Emanuel 4. Grell

2.2. Data and Experimental Design

The South Asia domain was organized for the regional study under WCRP CORDEX experiment (Giorgi et al. 2008). For ISM study, the South-Asia CORDEX domain (22°S–50°N and 10°E–130°E) has been chosen for RegCM-4.3 simulation. To better represent the responses of climate dynamics associated with the atmospheric convection and topographical complexity, it has been tried to conduct the RegCM-4.3 simulations at 0.5° × 0.5° resolution. The model-simulated daily OLR, MSLP, and the wind at 850 hPa are used to simulate the synoptic pattern associated with active/break phases of ISM. The initial conditions and boundary conditions (ICBC) with lateral boundary forcing are derived in 6 hourly fields from EIN15 reanalysis. These boundary conditions are available at 1.5° horizontal resolution and 37 vertical levels. The model-simulated daily data have been initialized from the 1st of May and integrated up to the 1st October for each of 25 years (1986–2010) time duration. In the present study, four individual CPSs such as Grell, Emanuel, Mix98 (Grell over the ocean, Emanuel over land) and Mix99 (Grell over land, Emanuel over the ocean) are considered. These CPSs are forced with the OISST in weekly pattern (OI_WK) with 1° × 1° resolution (Reynolds et al. 2002), obtained from NOAA. The detailed description of different CPSs in terms of the trigger conditions and closure assumptions is provided in Table 2.

To carry out the experiment, the active/break spells are considered from National Climate Centre (NCC) Research Report (2013) by IMD and treated as observational facts. The total numbers of active and break spells during the study period are 49 and 39 which are made up of 203 active days and 225 break days, respectively. OLR data of NOAA, MSLP of NCEP, and the wind at 850 hPa of EIN15 reanalysis over the considered domain are used for comparison with simulated pattern. The model-simulated results are extensively analyzed to find out the predictive skill in simulating the active/break phases of ISM over 71°E–83°E and 21°N–28°N which closely lies on the core monsoon zone of Rajeevan et al. (2010). For sensitivity analysis and verification, model-simulated parameters in the course of the active/break spells are compared with observed/reanalysis datasets. The data distributions are verified by the two tailed Q–Q plot (Wilk and Gnanadesikan 1968) in which the first quantile stands for observe/reanalyze data distribution and the CPS data distribution is placed in second quantile. For the good agreement in model validation, Taylor Diagram (Taylor 2001) is considered which represents the area averaged (over core monsoon region) temporal CC, SD and RMSE in one visual framework for 25 years period. For the sake of hand on circulation process during active/break phase, the anomaly of active/break phase from the seasonal mean and the anomaly between active and break phase are also displayed. For spatial distribution pattern validation, the spatial pattern CC (time independent) of MSLP climatology during active/break phase has also been considered.

3. Results and Discussion

Analysis of the synoptic phenomena using different CPSs of RegCM-4.3 is considered using wind (850 hPa), OLR and MSLP parameters and has been presented in Figs. 1, 2, 3, 4, 5, 6, 7, 8 and 9, in which

Table 2

Features of CPSs in RegCM-4.3

	Emanuel	Grell
Trigger condition	Level of buoyancy is higher than the cloud base level	Lifted parcel attains moist convection
Assumption	Quasi-equilibrium of updraft	Fritsch–Chappell (FC) closure: available buoyant energy is released within a timescale typically on the order of 30 min
Precipitation scheme	One updraft + one downdraft	One updraft + one downdraft
References	Emanuel (1991)	Grell (1993)

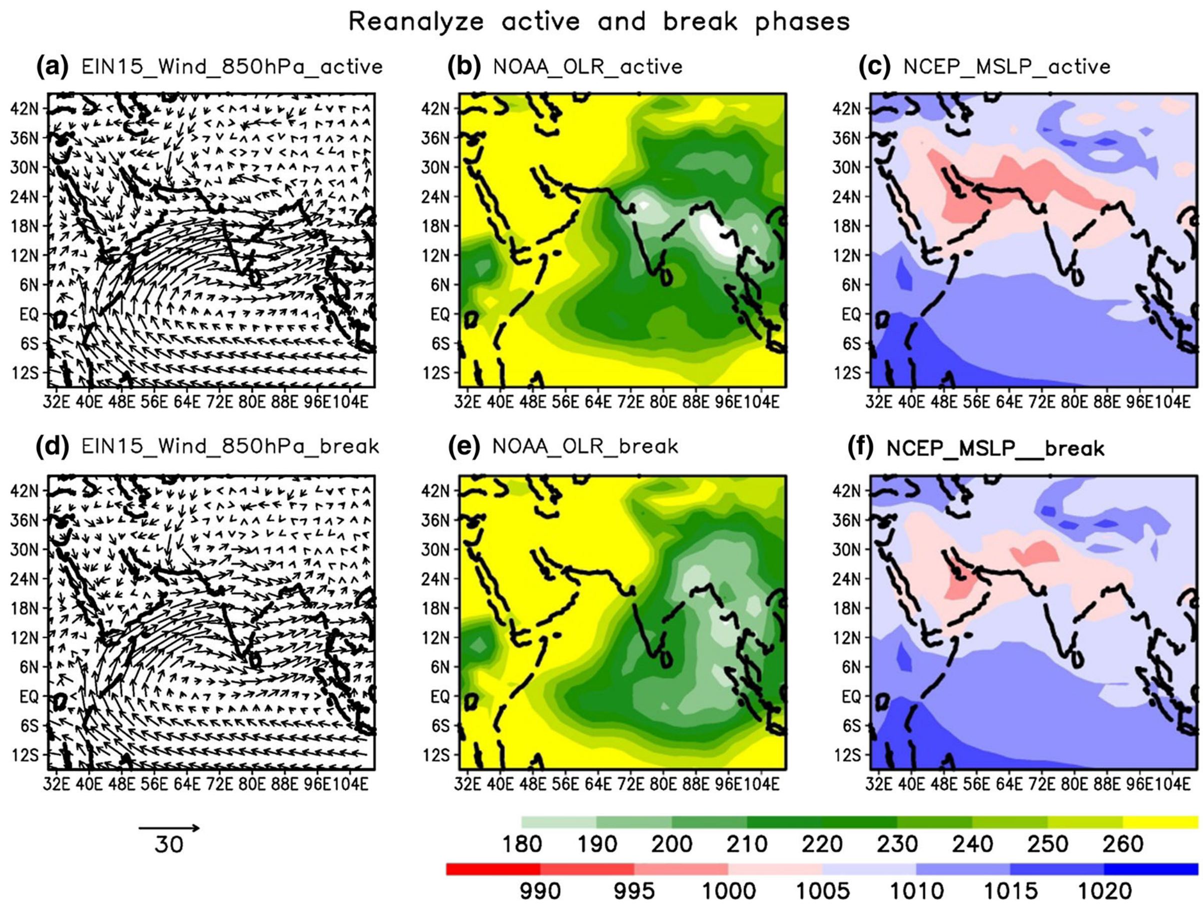

Figure 1

Circulation pattern of EIN15-wind (850 hPa), NOAA-OLR and NCEP-MSLP during (**a**–**c**) active and (**d**–**f**) break phases of ISM. The spatial pattern is based on the composite during the phases for 25-year time duration (1986–2010)

monsoon circulation in regular pattern along with the anomaly distribution has been considered. The model verification and validation have been statistically supported at the end of this section.

3.1. Monsoon Circulation During Active/Break Phase

Monsoon circulation during active/break spells is studied by considering the composite of OLR, MSLP, and the wind fields at 850 hPa. Model-simulated RegCM output with four different CPSs (Grell, Emanuel, Mix98 and Mix99) is compared with reanalysis datasets for 25 years climatology period. For the study of different phases of monsoon, the core monsoon zone considered between 71°E–83°E and 21°N–28°N which nearly lies on the monsoon region of Rajeevan et al. (2010). The spatial distribution of composite OLR, MSLP, and wind distribution (850 hPa) during active (Fig. 1a–c) and break (Fig. 1d–f) phases has been obtained from EIN15, NOAA and NCEP, respectively. It is observed that a very strong zonal wind is passing through the core monsoon zone of India during the active phase (Fig. 1a). The distributions of OLR shrinking during active phase are presented in NOAA-OLR (Fig. 1b). At the same time, a pressure belt of average of 995–1005 hPa is noticed over the Monsoon Convergence Zone (MCZ) (Fig. 1c). A low pressure system of less than 995 hPa is noted during the active period of monsoon over the core monsoon zone. The monsoon trough of MSLP (value 995–1005) is very

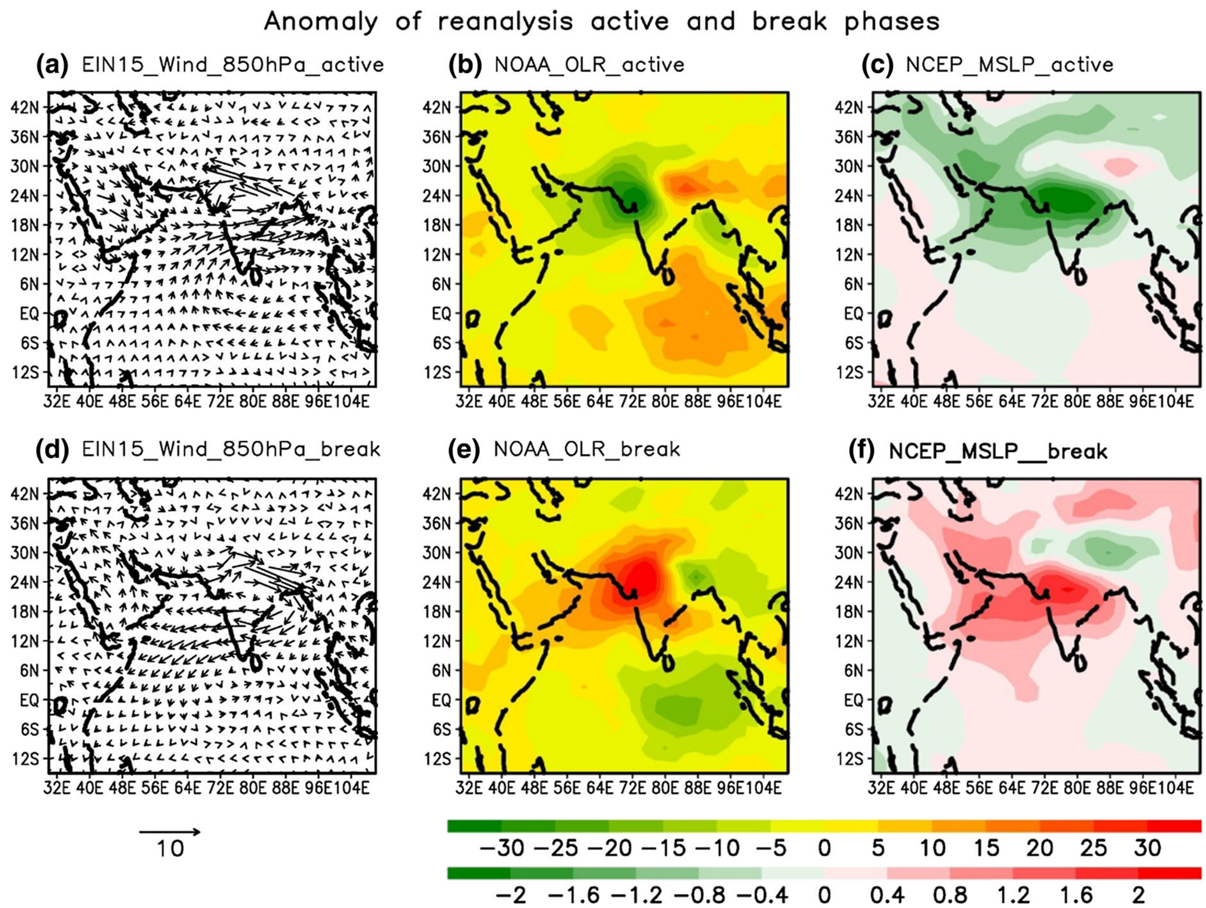

Figure 2

Spatial anomaly pattern of EIN15-wind (850 hPa), NOAA-OLR and NCEP-MSLP during the active and break phases of monsoon during 1986–2010. The anomalies during (**a**–**c**) active and (**d**–**f**) break phases have been considered by subtracting the climatology seasonal mean from the respective phases of ISM

prominent near the foot of Himalaya during these days. The region of low MSLP covers a very large area over western India, Pakistan, Afghanistan and middle-east Asia during the active phase. The reverse is observed in wind, OLR and MSLP during the break phases of monsoon. The low level jet shows a slight southward deflection in wind direction over the core monsoon region during break phase (Fig. 1d). The rising in the OLR distribution over the core monsoon region is showing very high (Fig. 1e) and the monsoon trough has been shifted from the central India to the Himalayan foot hills (Fig. 1f). A small region of low MSLP prevails over Northwest India, Pakistan and Saudi Arabia during this phase. For the sake of hand about the phase dynamics during active and break, the anomaly from seasonal mean JJAS has been considered for the respective parameters in Fig. 2a–f. A clear and opposite progression is observed in the anomalies during active and break phases. A strong wind circulation blows over the core monsoon region during active phase than seasonal mean wind circulation during monsoon (Fig. 2a)

Figure 3 ▶

OLR circulation pattern and the anomaly of different CPSs of RegCM during (**a**–**h**) active and (**i**–**p**) break phases of ISM during 1986–2010. The anomalies during active and break phases have been considered by subtracting the climatology seasonal mean from the respective phase and CPS

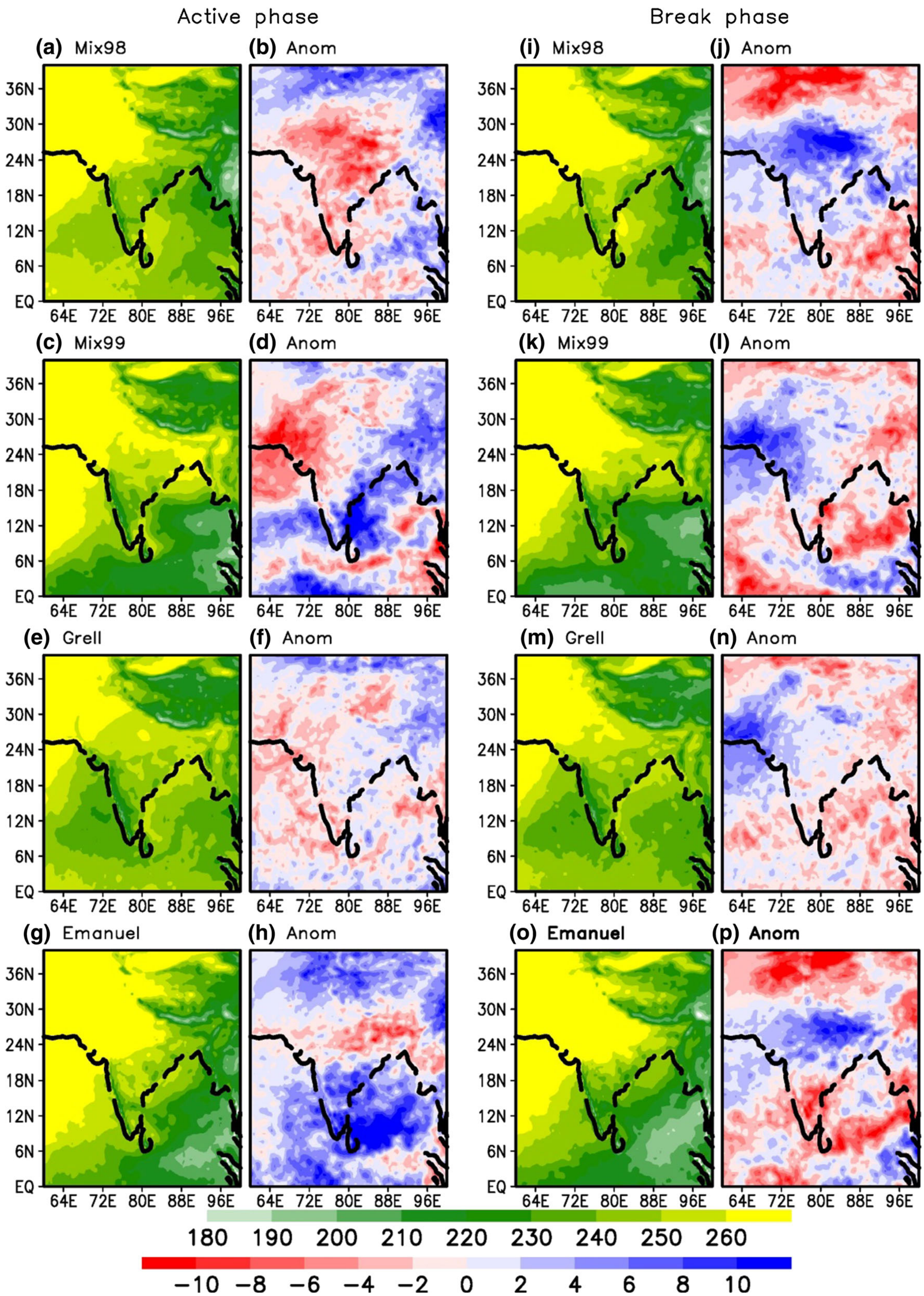
Active phase
Break phase
(a) Mix98
(b) Anom
(c) Mix99
(d) Anom
(e) Grell
(f) Anom
(g) Emanuel
(h) Anom
(i) Mix98
(j) Anom
(k) Mix99
(l) Anom
(m) Grell
(n) Anom
(o) Emanuel
(p) Anom
36N
30N
24N
18N
12N
6N
EQ
64E 72E 80E 88E 96E
180 190 200 210 220 230 240 250 260
−10 −8 −6 −4 −2 0 2 4 6 8 10

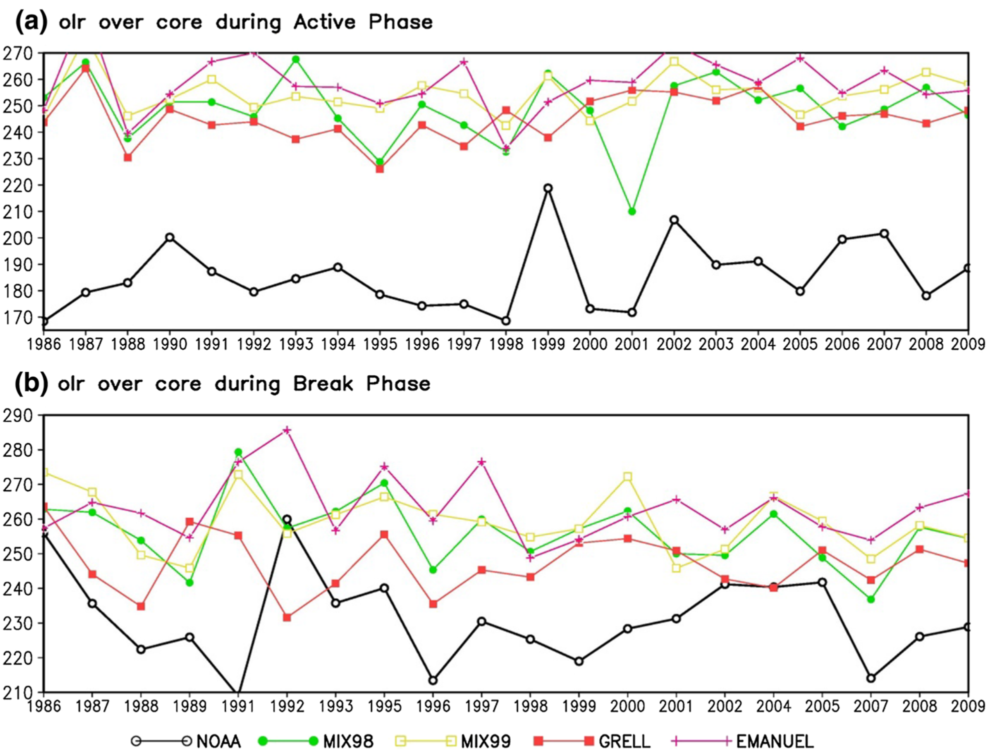

Figure 4
Temporal series of composite OLR of NOAA and model-simulated CPSs during active and break phases during 1986–2010

which becomes weaker during the break phases and speed of wind over the core monsoon region is half of the active phase (Fig. 2d) (Varikoden 2006). Fig. 2b, d represents the OLR anomaly from the seasonal JJAS OLR mean during the active and break phases. A vice versa OLR distribution is represented from the anomaly plot. Region over core monsoon zone represents low (high) OLR during active (break) phase and, therefore, a sharp negative (positive) anomaly is observed in OLR anomaly distribution (Fig. 2b/d). The most prominent feature during active and break phases is the shifts of monsoon trough over core monsoon zone to Himalayan foot hills which are clearly represented in Fig. 2c, f. During active phase, the mean trough position shifts towards the core monsoon region (Fig. 2c) and during break it has been shifted towards the foot hill Himalaya (Fig. 2f).

Convection has an important role in the formation of cloud and the total cloud amount is inversely related to OLR which is the cause of excess or deficit of rainfall (Raju et al. 2009). Figure 3 represents the OLR distribution during active/break phases and its anomaly from the seasonal mean (JJAS) for all the considered CPSs. The CPS-simulated RegCM performance during active/break phases over Indian core monsoon zone for the OLR (Fig. 3a–p) is compared with reanalyzed datasets (Figs. 1 and 2). The spatial OLR distribution and its anomaly from the seasonal mean simply represent the proxy of rainfall over the region. In other words, positive/negative anomalies of OLR are the cause of negative/positive anomaly of rainfall. Thus, OLR is a good proxy for inferring the rainfall activity associated with the tropical convection, i.e., and that is why the identification of different phases of monsoon using OLR is greatly facilitated to capture conspicuous nature of phase's anomaly

Figure 5 ▶
Circulation pattern MSLP and the anomaly of different CPSs of RegCM during (**a**–**h**) active and (**i**–**p**) break phases of ISM during 1986–2010. The anomalies during active and break phases have been considered by subtracting the climatology seasonal mean from the respective phase and CPS

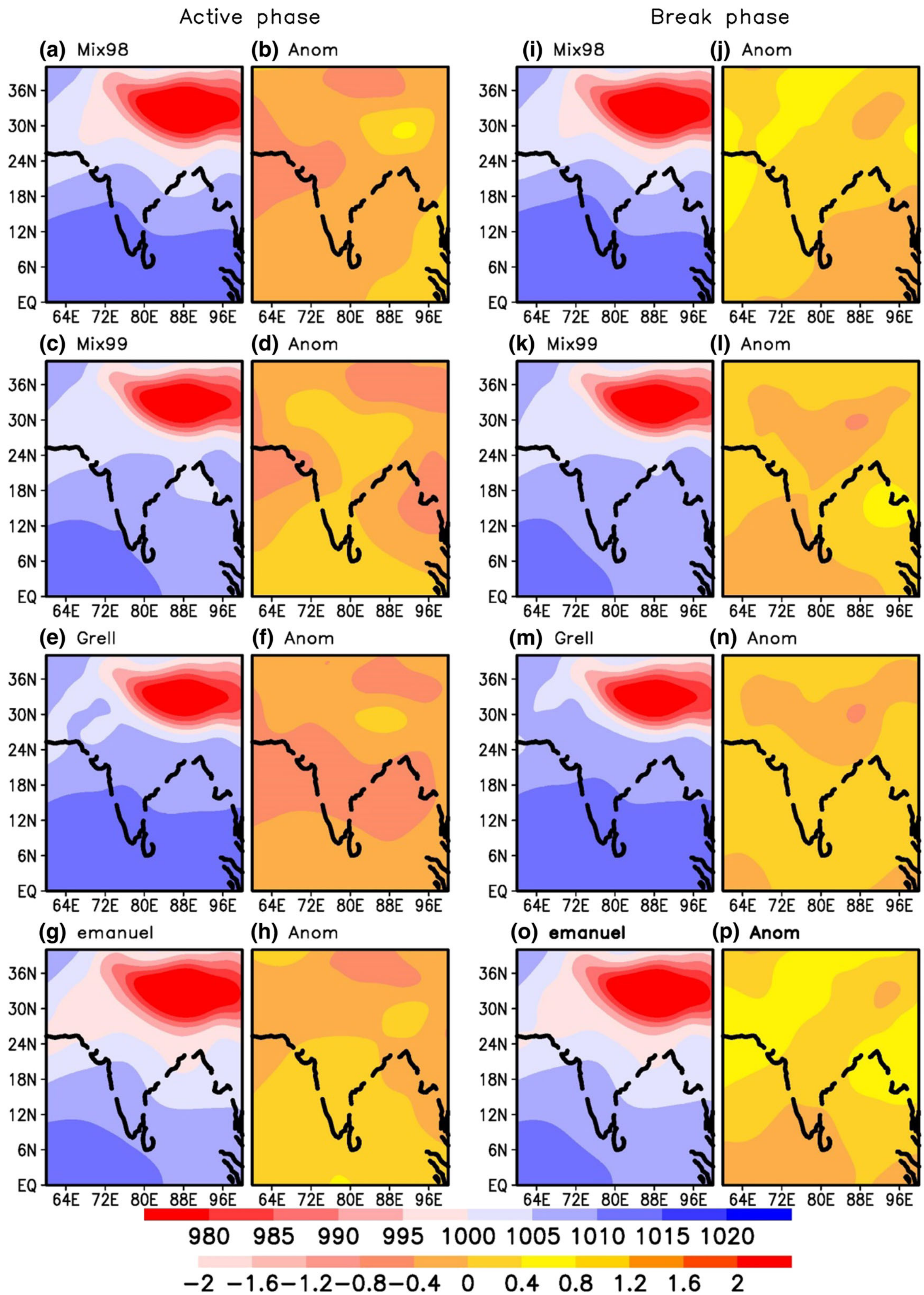
Active phase
Break phase
(a) Mix98
(b) Anom
(c) Mix99
(d) Anom
(e) Grell
(f) Anom
(g) emanuel
(h) Anom
(i) Mix98
(j) Anom
(k) Mix99
(l) Anom
(m) Grell
(n) Anom
(o) emanuel
(p) Anom
36N 30N 24N 18N 12N 6N EQ
64E 72E 80E 88E 96E
980 985 990 995 1000 1005 1010 1015 1020
−2 −1.6 −1.2 −0.8 −0.4 0 0.4 0.8 1.2 1.6 2

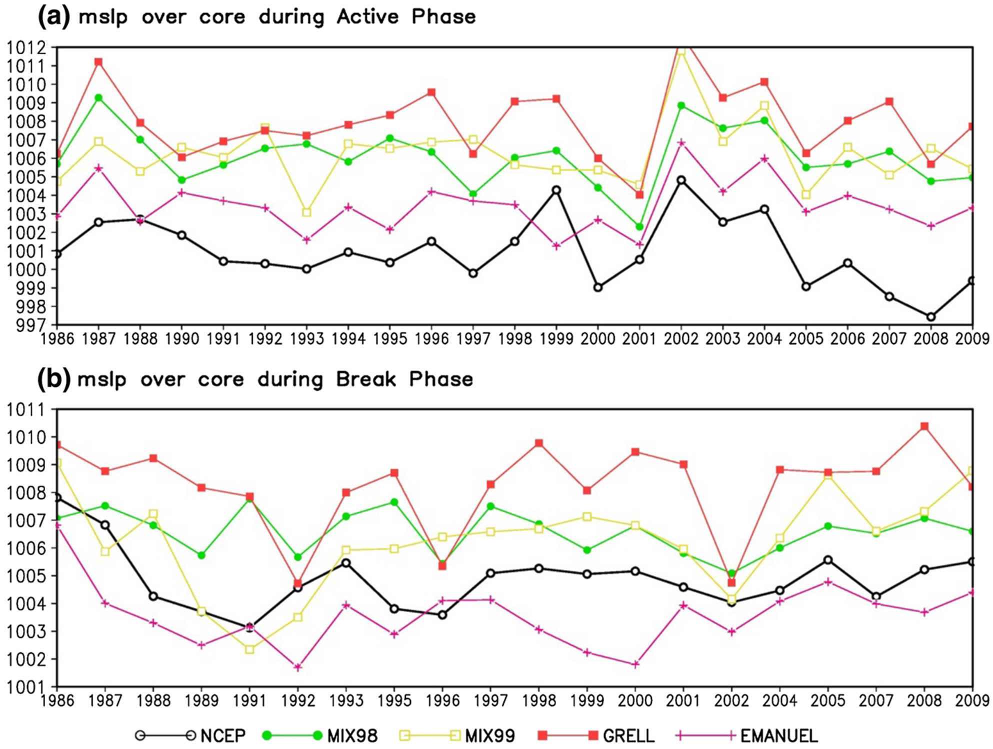

Figure 6
Temporal series of composite MSLP of NCEP and model-simulated CPSs during active and break phases during 1986–2010

(Krishnan et al. 2000). It is observed that the spatial distributions of all CPSs (Fig. 3a–p) have been more or less following the pattern of reanalysis OLR. During active (break) phase, the formations of OLR over the core monsoon region are represented well in Mix98 CPS but the anomaly shows a positive (negative) OLR for the phases. OLR distribution and the anomaly in the CPS Mix99 are following the pattern of NOAA (Fig. 2). It is also observed that the Mix99 CPS very closely follows the NOAA-OLR over the surrounding area of western and north-western part of India. The positive/negative anomaly over the regions is very prominent in relative to the NOAA during active/break phases. The Grell CPS is weak in OLR distribution simulation during active/break phases as the anomaly from the seasonal mean shows less which represents non-variation of OLR during the phases. Emanuel CPS is failed to capture the spatial distribution over the Western and North-Western part of India during the phases. Previous study by Raju et al. (2009) has found the same

Figure 7 ▶
Spatial pattern correlation-coefficient (CC) of CPS's and NCEP MSLP climatology pattern for active and break phases

mechanism during active/break of monsoon. The temporal composite OLR distributions during active/break phases over the core monsoon region are considered in Fig. 4a, b where Fig. 4a stands for the distribution during active phases and Fig. 4b represents the break phases for reanalyzed and model-simulated output. The temporal distribution represents a very high overestimation in OLR for all the CPSs with respect to reanalysis during active phase (Fig. 4a). During break phases, the data distribution follows the NOAA-OLR for the 25 years period (Fig. 4b). The above analysis may conclude in support of the Mix99 CPS by following the spatial pattern of NOAA with the overestimation in OLR over the region. The overestimation in model CPSs' OLR is due to the lack of wind circulation speed in model simulation which was carried forwarded from

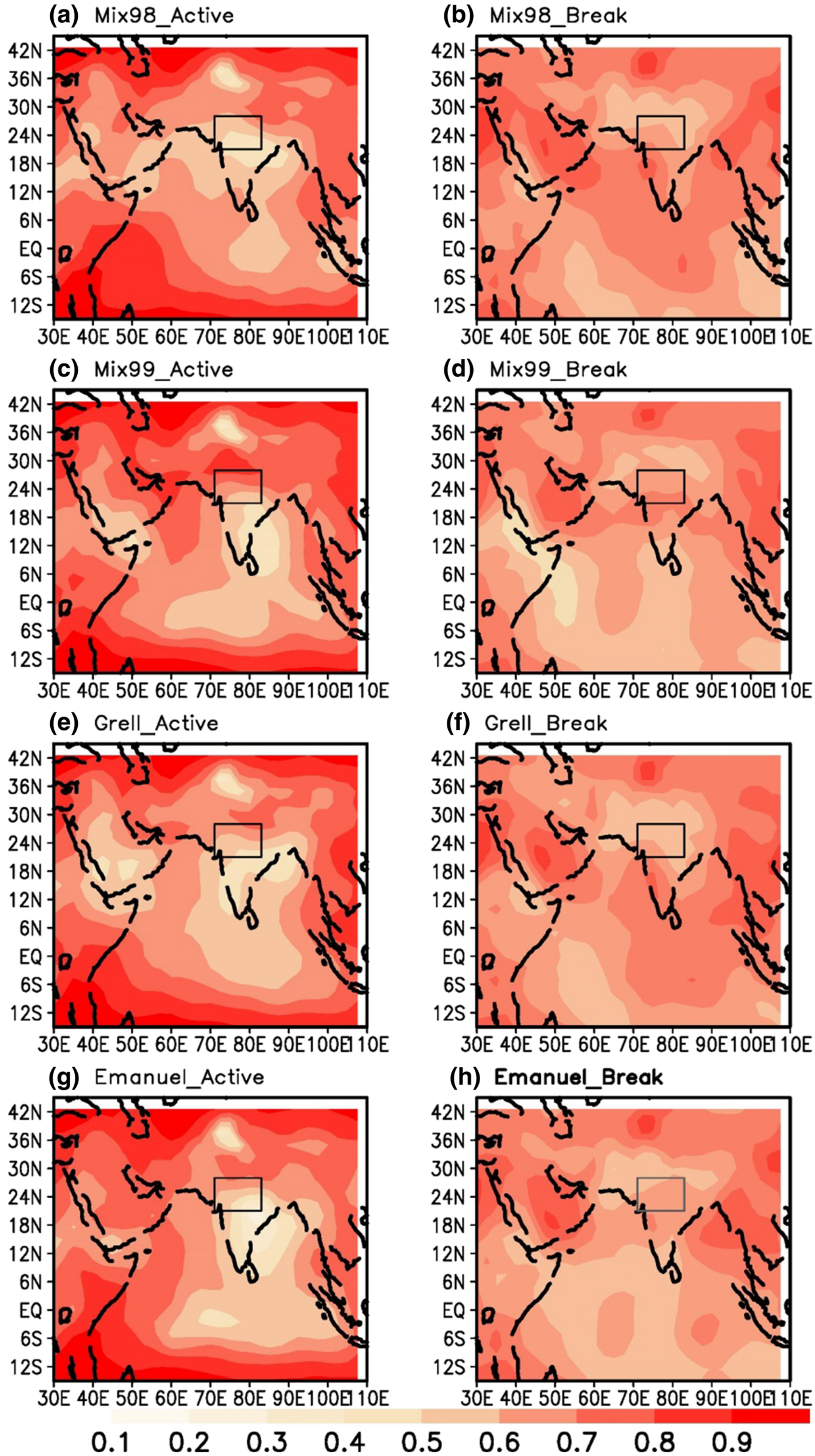
(a) Mix98_Active
(b) Mix98_Break
(c) Mix99_Active
(d) Mix99_Break
(e) Grell_Active
(f) Grell_Break
(g) Emanuel_Active
(h) Emanuel_Break
42N
36N
30N
24N
18N
12N
6N
EQ
6S
12S
30E 40E 50E 60E 70E 80E 90E 100E 110E
0.1 0.2 0.3 0.4 0.5 0.6 0.7 0.8 0.9

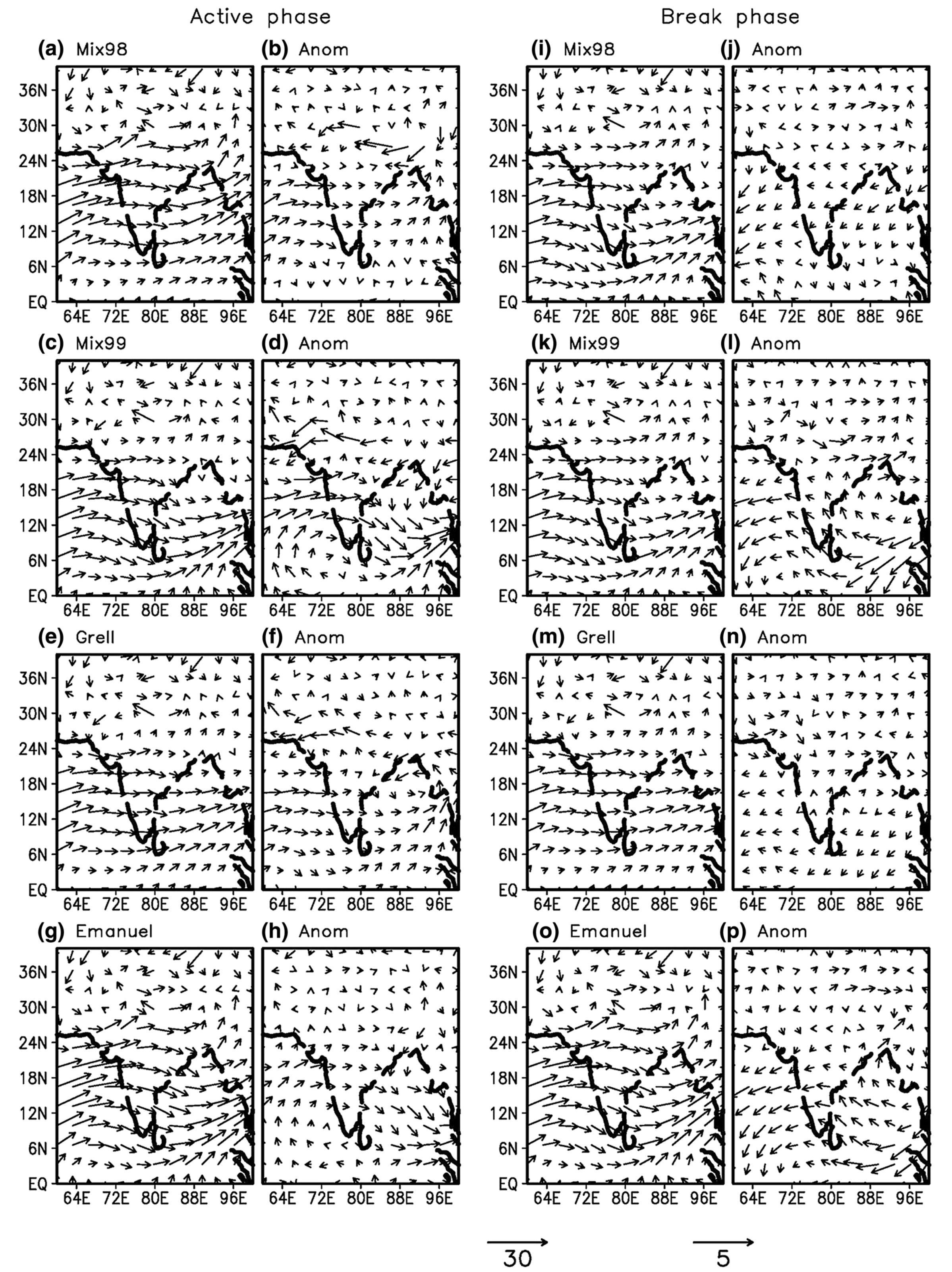
Active phase
Break phase
(a) Mix98
(b) Anom
(c) Mix99
(d) Anom
(e) Grell
(f) Anom
(g) Emanuel
(h) Anom
(i) Mix98
(j) Anom
(k) Mix99
(l) Anom
(m) Grell
(n) Anom
(o) Emanuel
(p) Anom
36N
30N
24N
18N
12N
6N
EQ
64E 72E 80E 88E 96E
30
5

◀Figure 8
Wind circulation at 850 hPa and the anomaly of different CPSs of RegCM at the same height during (**a**–**h**) active and (**i**–**p**) break phases of ISM during 1986–2010. The anomalies during active and break phases have been considered by subtracting the climatology seasonal mean from the respective phase and CPS

the EIN15 data over the core monsoon region during active phase. This is the cause behind not propagating of OLR from the central India and model simulated OLR distribution are showing high value over the region during the phase (Ghosh et al. 2018).

An inverse correlation between precipitation and MSLP is observed by Li et al. (2005), Allan and Haylock (1993) illustrated that the low (high) zone of MSLP is in relation to high (low) rainfall over a specific area in a certain condition. In Fig. 5a–p, the low pressure area covers the MCZ in the CPSs simulation during active phase and during break phase; the development of low pressure observed more prominently over the MCZ has been depicted in the spatial distribution. The spatial distributions of model simulation have been compared with the reanalyzed MSLP during active and break phases (Fig. 1). Trough of MSLP over the MCZ shows the value of 995–1000 hPa during active phase and 1000–1005 hPa during break of ISM has also been observed in the CPSs. The distribution is more observable in anomaly distribution in Fig. 5. The appearance of monsoon trough during active phase and shifting toward the Himalayan foothills during break phase with the disappearances from core monsoon zone (Taraphdar et al. 2010; Ramamurthy 1969; Rao 1976) are well depicted in the Mix99 and Grell CPSs during the respective phases. This disappearance of monsoon trough is also evident in the anomaly pattern during active/break phases of monsoon. Mix98 and Emanuel are simulating less in comparison to the other schemes. The time series analysis for MSLP is also considered over the specified region in which distribution matches with

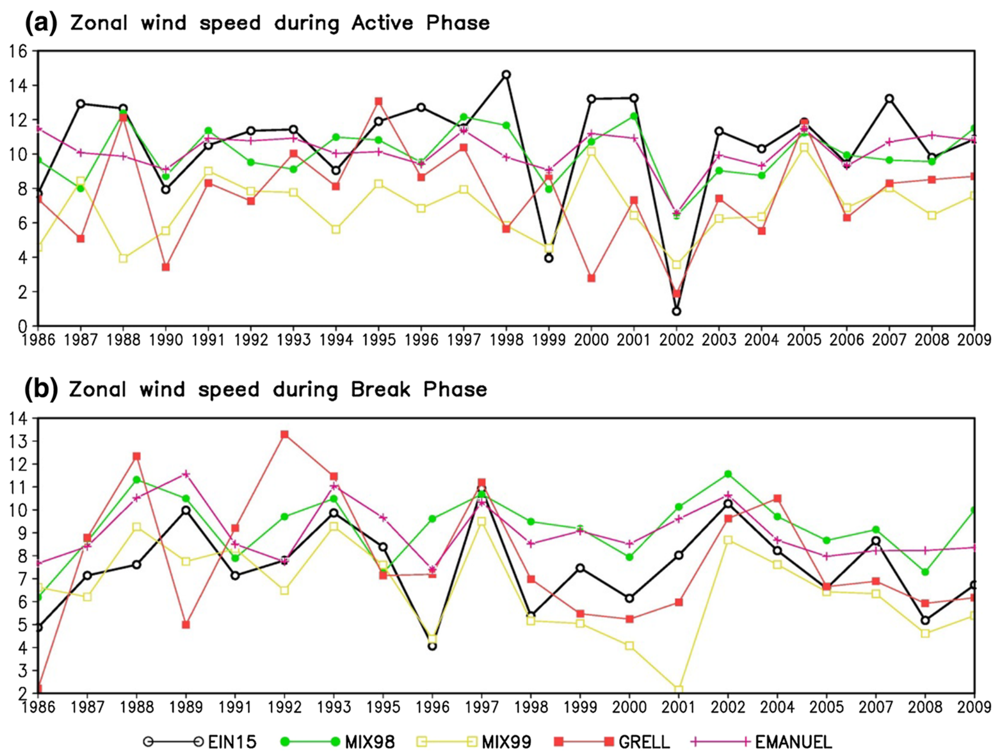

Figure 9
Temporal series of composite zonal wind of EIN15 and model-simulated CPSs at 850 hPa during active and break phases during 1986–2010

the spatial pattern itself and with the pattern of NCEP reanalysis (Fig. 6). In this temporal distribution, the Emanuel and Mix99 are closely resemblance with the reanalyzed datasets and Grell scheme shows a slight overestimation during active and break phases of monsoon. Further, it has been tried to obtain the correlation-coefficient (CC) of spatial pattern of MSLP climatology distribution for the CPSs with respect to NCEP reanalysis during active and break phase (Fig. 7). It is observed that the MSLP distributions of all CPSs are well correlated during active phases and break. Spatial distribution of CC in active phases goes up to 0.7 over some parts of the core monsoon zone (rectangle box) and for break phases it is up to 0.6. Detailed analyses of statistical scores have been considered in further discussion.

The distribution of wind at 850 hPa using RegCM-4.3 is shown in Fig. 8a–p and compared with the EIN15 reanalysis data (Figs. 1 and 2). This distribution shows that a strong low level westerly comes across the Somalia and blows through the central India during the active phase of monsoon. The wind circulation at 850 hPa is stronger with respect to the seasonal circulation which is observed from the anomaly distribution from seasonal mean during the active phase. During break phase, a weak westerly wind is prevailing over the north of the Indian region and shifts towards the south. The deviation of wind direction from the core monsoon zone to the south-east India is presented well in CPSs Mix99 and Emanuel during break phases which can be observed from the break phase anomaly. From the figures, it can be described that during break phase the wind circulates with the half speed of active phase wind circulation (Varikoden 2006) and, therefore, wind circulation anomaly during break phase represents outwards with respect to seasonal wind circulation speed. This wind circulation during the break phase is well observed by Mix98, Mix99 and Emanuel CPSs. The Grell scheme seemed to be successful over the plain areas (Sardar et al. 2012); therefore, due to the topographical complexity over Indian land region, Grell CPS is not able to capture wind circulation mechanism during active/break phases. The better performance of Emanuel CPS may be due to the triggering factor in the CPS due to the uplift of a parcel (Elguindi et al. 2011) over a region of complex topography. From the active to break phase of monsoon, a substantial decrease of wind speed is also observed in the anomaly pattern. A strong wind speed in the reanalysis data (earlier discussion) as well as in different CPSs is observed during the active phase and the opposite formulation is noticed during break. For the sake of hands, the temporal distribution of zonal wind speed during the phases with different CPSs with respect to reanalysis is considered in Fig. 9a, b. In this figure, the zonal wind speed of four CPSs follows the pattern of EIN15 reanalysis during active (Fig. 9a) as well as during the break phases (Fig. 9b) of monsoon. The CPSs distribution completely follows the EIN15 wind distribution and an average difference in zonal wind speed of 3 ms^{-1} is noticed between active to break phase zonal wind circulation. It is also observed that the EIN15 and model-simulated zonal wind speed over the core region show very less difference between active and break phase in contrast to the study of Varikoden (2006). Ghosh et al. (2018) have illustrated that the RegCM-simulated output is forced to simulate underestimation in zonal wind circulation speed due to lack of wind speed in EIN15 datasets over some specified region which was carried forward during model simulation. The convection is significantly enhanced/reduced with the strong/weak zonal wind flow over the Indian region during active/break phases of ISM (Annamalai and Slingo 2001). Therefore, in CPSs, the weak zonal wind circulation is failed to lift the OLR parcel from the core monsoon region and is the cause behind the overestimation in OLR simulation over the region (Ghosh et al. 2018).

3.2. *Spatial Distribution of Active/Break Phase Anomalies*

Earlier section has briefly discussed the large-scale intra-seasonal variation and the simulation over core monsoon region. This section has been elaborated the anomaly distribution of active and break phases of monsoon. Figures 10a, b and 1a–h represent the spatial anomaly distribution of reanalysis and CPSs, respectively. The anomaly has been processed by deducting the active phase from break phase. A deep clarification in the circulation process of OLR and MSLP in synaptic scale has been tried by

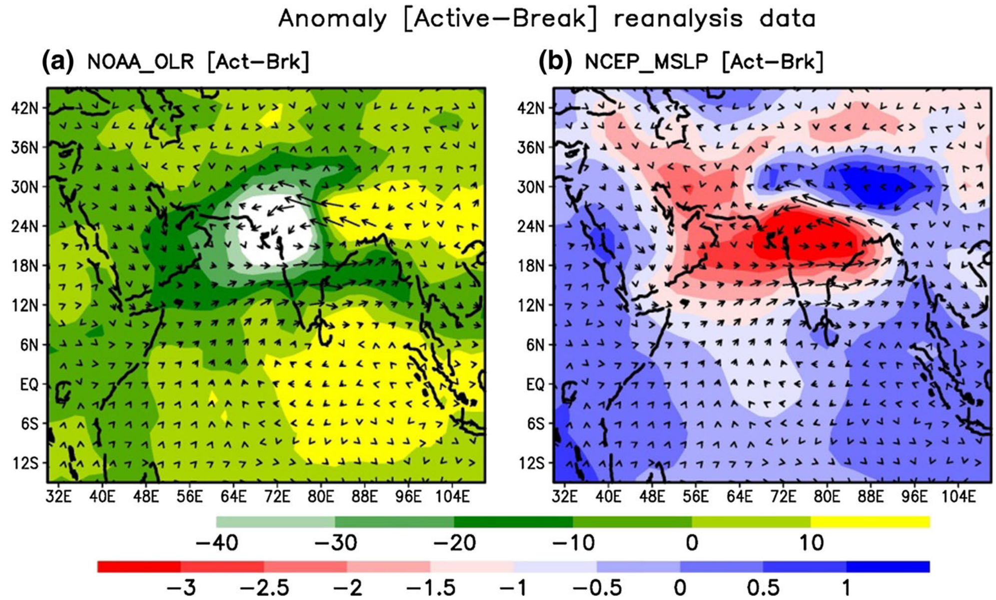

Figure 10
Anomaly (active–break phase) of reanalyzed OLR, MSLP and wind (850 hPa) propagation during 1986–2010

superimposing the wind circulation at 850 hPa over the considered parameters. A large negative anomaly in OLR distribution ($< -30\ \mathrm{Wm}^{-2}$) over the MCR and the core monsoon zone is noticed (Fig. 10a) which represents the high OLR value over the region during break phase than active days. At the same time, a negative pressure belt is raised over the region of negative OLR anomaly (Fig. 10b). The positive anomaly over the Himalayan region is also noticed during the period. A cyclonic wind circulation is covering the respective zone. In other words, the low OLR and low MSLP along with high speed jet at 850 hPa are the result of active rainfall and reverse for break phase. These are the prominent dynamics for active and break phases of monsoon. Figure 11a–h represents the anomaly of active/break phase with four CPSs. The negative distribution of OLR and MSLP anomaly pattern along with the cyclonic wind circulation over MCR and the core monsoon zone of India is well simulated by CPS Mix98 and Mix99 (Fig. 11a–d). Although, a mild anomaly value is observed over the respective north-west and west part of India in comparison to Fig. 10a, b. In this respect, it is also observed that the Mix98 scheme (Fig. 11a, b) simulates the features over the core monsoon region which is slightly displaced from the reanalyzed negative anomaly region (Fig. 10a, b). This regional feature is well simulated with the Mix99 CPS (Fig. 11c, d). The closer assumption of Grell and Emanuel CPSs regarding the simulation of the features is very faint. From the analysis, it is also observed that the deep negative MSLP anomaly is being simulated slight far from the actual region in respect to reanalyse. To find out the uncertainty behavior of different CPSs, the sensitivity analyses are considered for statistical score.

3.3. *Verification and Validation*

For verification and validation, probability distribution (Q–Q plot) and Taylor Diagram are considered which assessed the relative performance of model with respect to baseline (reanalysis/observation dataset) (ParthSarthi et al. 2015, 2016).

Q–Q plot is the probability plot to compare the shape of distribution between two data series with a graphical method by plotting their quantiles against each other (Wilk and Gnanadesikan 1968). Q–Q plots can also be used to compare a collection of data or theoretical distributions (Singh et al. 2014). In this

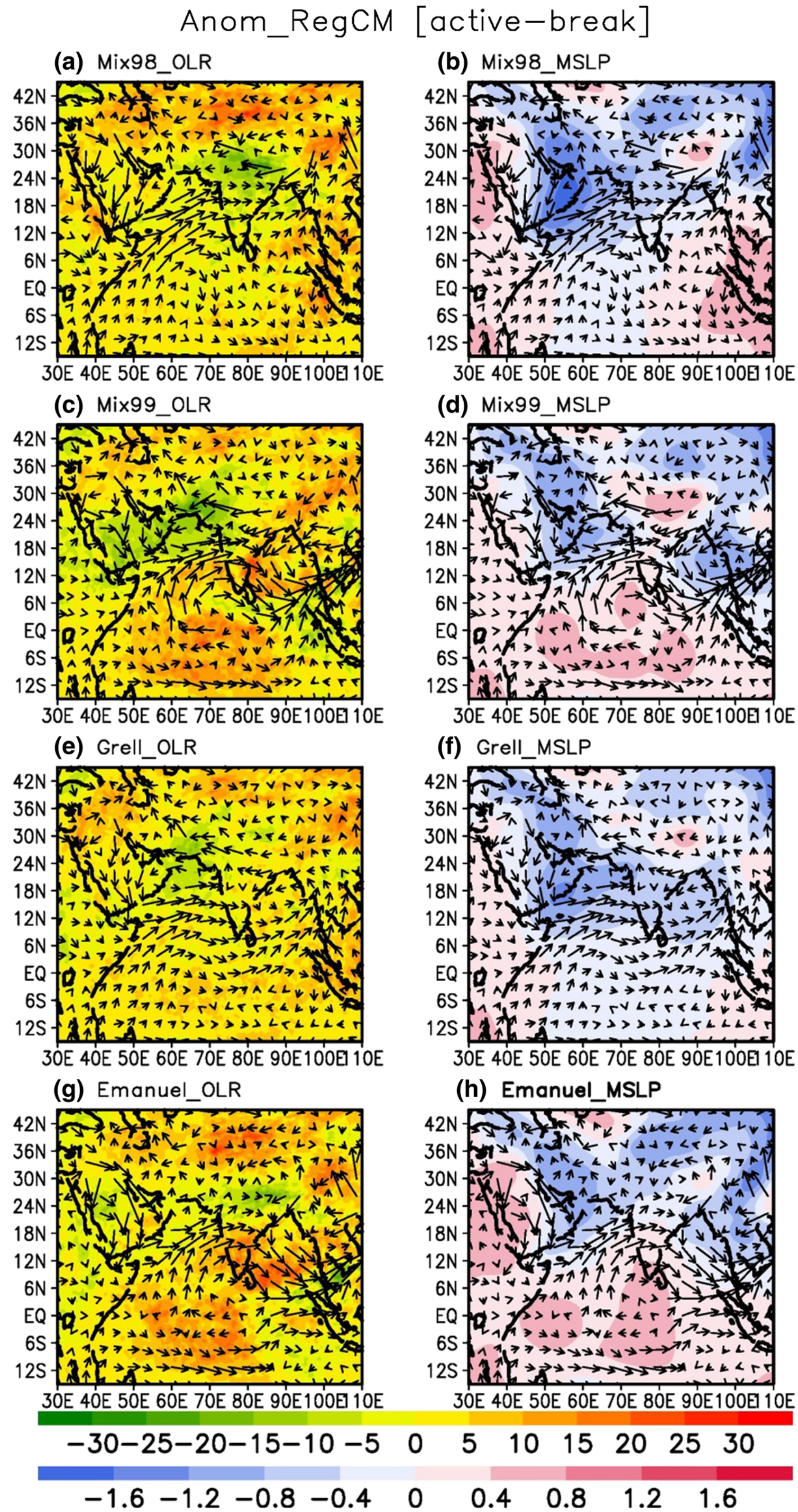
Anom_RegCM [active−break]
(a) Mix98_OLR
(b) Mix98_MSLP
(c) Mix99_OLR
(d) Mix99_MSLP
(e) Grell_OLR
(f) Grell_MSLP
(g) Emanuel_OLR
(h) Emanuel_MSLP
42N 36N 30N 24N 18N 12N 6N EQ 6S 12S
30E 40E 50E 60E 70E 80E 90E100E110E
−30 −25 −20 −15 −10 −5 0 5 10 15 20 25 30
−1.6 −1.2 −0.8 −0.4 0 0.4 0.8 1.2 1.6

◀ Figure 11
Anomaly (active–break phase) of different CPS's OLR, MSLP and wind (850 hPa) propagation during 1986–2010

study, Q–Q plots are used to compare the CPS's performance as a nonparametric approach and their underlying distributions are distributed with respect to reanalyze datasets (Fig. 12a–l). These distributions provide an assessment of goodness of fit with the graphical representation between model and baseline data distribution. In the figures, red scatters indicate the distribution for active spells and blue scatters indicate the distribution for break spells. The points in *x* and *y* axes in Fig. 12a–l correspond to one of the quantiles of the second distribution (*y* coordinate) and plotted against the same quantiles of the first distribution (*x* coordinate). If CPS and reanalysis data distributions behave in similar manner, then the points are laid approximately on the line with 45° angle and if the distributions are linearly related, then the scatters are laid approximately on a line, but it is not necessarily to be laid on the line $y = x$. Here, the first quantile represents the distribution for observe/reanalyze data and the second quantile stands for the model-simulated output. In the figure, the model-simulated OLR distribution during active and break phases is overestimated with respect to the second quantile (Fig. 12a–d). It is also observed that the OLR distribution in Mixed CPSs and Grell CPS is performing well where the Emanuel CPS shows more deviation than others. Figure 12e–h represents the MSLP distribution between model and observed quantile which indicate good performance in Mixed and Emanuel CPSs. Although, Emanuel CPS shows a little bit closer in MSLP distribution with the second quantile than other CPSs, still the progression of MSLP from core monsoon region to Himalaya foothill (briefly discussed in Sects. 3.1 and 3.2) is well observed in Mix99 CPS. In this figure, MSLP distribution in Mix99 clearly shows the opposite progress during active and break days. The zonal wind distribution of EIN15 and model-simulated quantiles is displayed in Fig. 12i–l. The visual framework of Q–Q distribution represents the goodness of fit of model-simulated zonal wind distribution

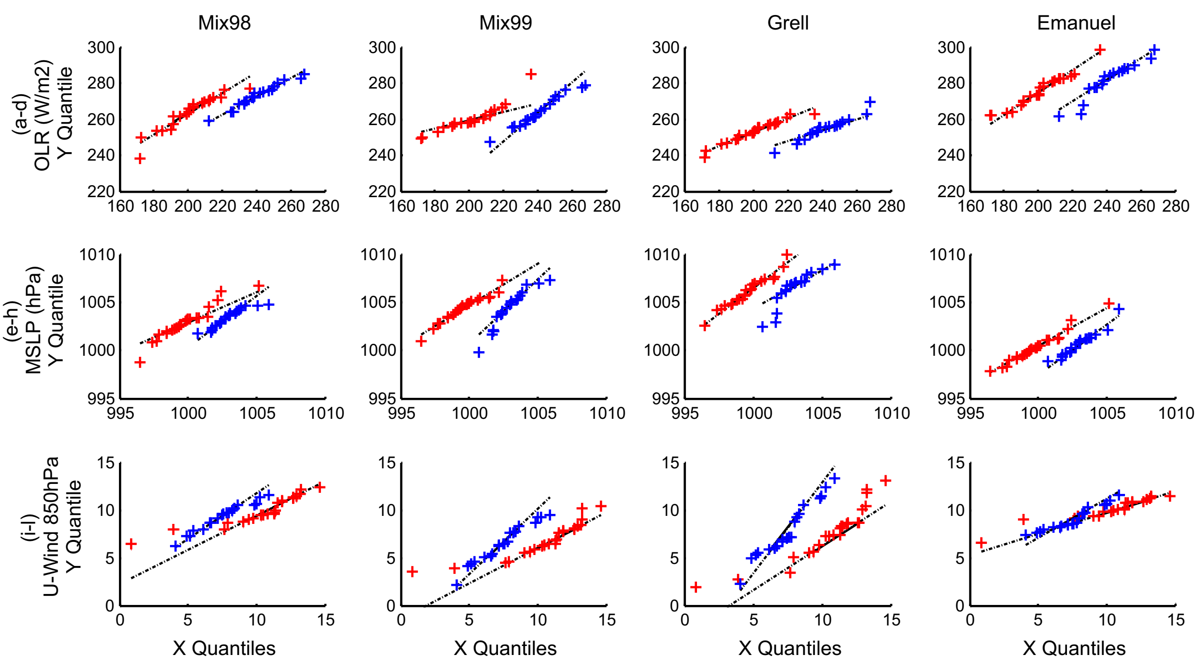

Figure 12
Quantile–Quantile (Q–Q) plots for active and break phases of ISM over the core monsoon zone of India during 1986–2010. The red scatters represent the active spells and the blue represents break spells of monsoon

with the EIN15 distribution in Mix99 CPS, as the scatters lie with the abline with about 45° angle. Mix99 and other CPSs also represent about the equal speed in zonal wind speed over core monsoon region between active/break phases of monsoon. The justification behind the speed in zonal wind uncertainty during active and break phases is explicitly elaborated in Sect. 3.1. The Q–Q distribution shows clean and opposite phenomena in all the parameters by Mix99 CPS during model-simulated active and break days of monsoon which show relatively the actual progression in RegCM-simulated different parameters during the phases. Another interesting finding is that the model-simulated break phase distribution (for parameters OLR, MSLP and zonal wind) always shows better simulation than active phase simulation.

Taylor diagram shows the degree of likeness between observed and model-simulated active/break phases for 25 years time duration over the core monsoon region. The degree of likeness is determined by computing Pearson CC between CPSs and reanalysis data, RMSE of CPSs with respect to reanalysis data and SD of reanalysis as well as CPSs. When the CPSs have relatively high CC, low RMSE and least distribution of SD, the CPSs performance is close to reanalysis. Figure 13a–f represents the Taylor Diagram of different CPSs for active and break phases of ISM. The empty circle on positive x-axis represents the baseline of the reanalysis data and the bullets with different colors in the field area represent different CPSs which have been considered for this study. Figure 13a–c represents the model data validation during active phase for the parameters OLR, MSLP and zonal wind. The diagram shows a weak RegCM performance in OLR distribution (Fig. 13a) and a healthy relationship in MSLP (Fig. 13b) and zonal wind distribution (Fig. 13c) with respect to reanalyze the data. It is also observed that the Grell scheme represents weak performance with reanalyzed datasets in OLR and wind distribution. Although, CPS Emanuel is performing well in comparison to other CPSs for OLR and wind distribution but the overall performance of Mixed CPSs is very surprising by simulating the active phase very well. The performances of the considered parameters during break phases have been displayed in Fig. 13d–f. It seems that the Emanuel is performing well for all parameters. The mixed schemes are also showing their goodness of fit for the parameters during the break phase. For overall performance of RegCM-4.3 simulation during active/break phase, the CPS Mix99 and Emanuel perform well with relatively high CC, low RMSE with respect to reanalysis dataset and least SD. As all the CPSs show low statistical score for OLR simulation during active phase, simulation bias might be the possible cause for this irregular behavior. Previous study has shown better performance of Grell CPS over Indian land region (Mamgain et al. 2013) and Emanuel over the ocean (Bhatla and Ghosh 2015). The uncertainty behavior in model-derived OLR is due to the lack of zonal wind speed over the core monsoon region during the rainy phase which is not able to lift the OLR parcel from the central India and model shows large bias over the region (Ghosh et al. 2018). Another possible cause behind this behavior is the downdraft mass fluxes towards the state of quasi-equilibrium with the large-scale forcing. For Emanuel CPS, the updraft mass fluxes are represented as a vertical velocity which is determined by the amount of convective available potential energy and helps in turn to determine in such way to drive the mass fluxes towards the state of quasi-equilibrium with large-scale forcing. The downdraft mass fluxes are unique functions of the mass fluxes which are responsible for closeness with the system (Emanuel 1991).

Figure 13 ►

a–**c** Taylor Diagram of RegCM-simulated OLR, MSLP and zonal wind (850 hPa) performance with respect to observe/reanalyze during active phases of monsoon. The statistical distribution shows the performance of different CPSs over core monsoon zone for 25 years duration. **d**–**f** Taylor Diagram of RegCM-simulated OLR, MSLP and zonal wind (850 hPa) performance with respect to observe/reanalyze during break phases of monsoon. The statistical distribution shows the performance of different CPSs over core monsoon zone for 25 years duration

4. Conclusions

This study demonstrates the current understanding of Mix99 CPS performance as a best-suited CPS among RegCM-4.3 for simulation the intra-seasonal and interannual monsoon over core monsoon region. As a mass flux CPS scheme, Grell is generally

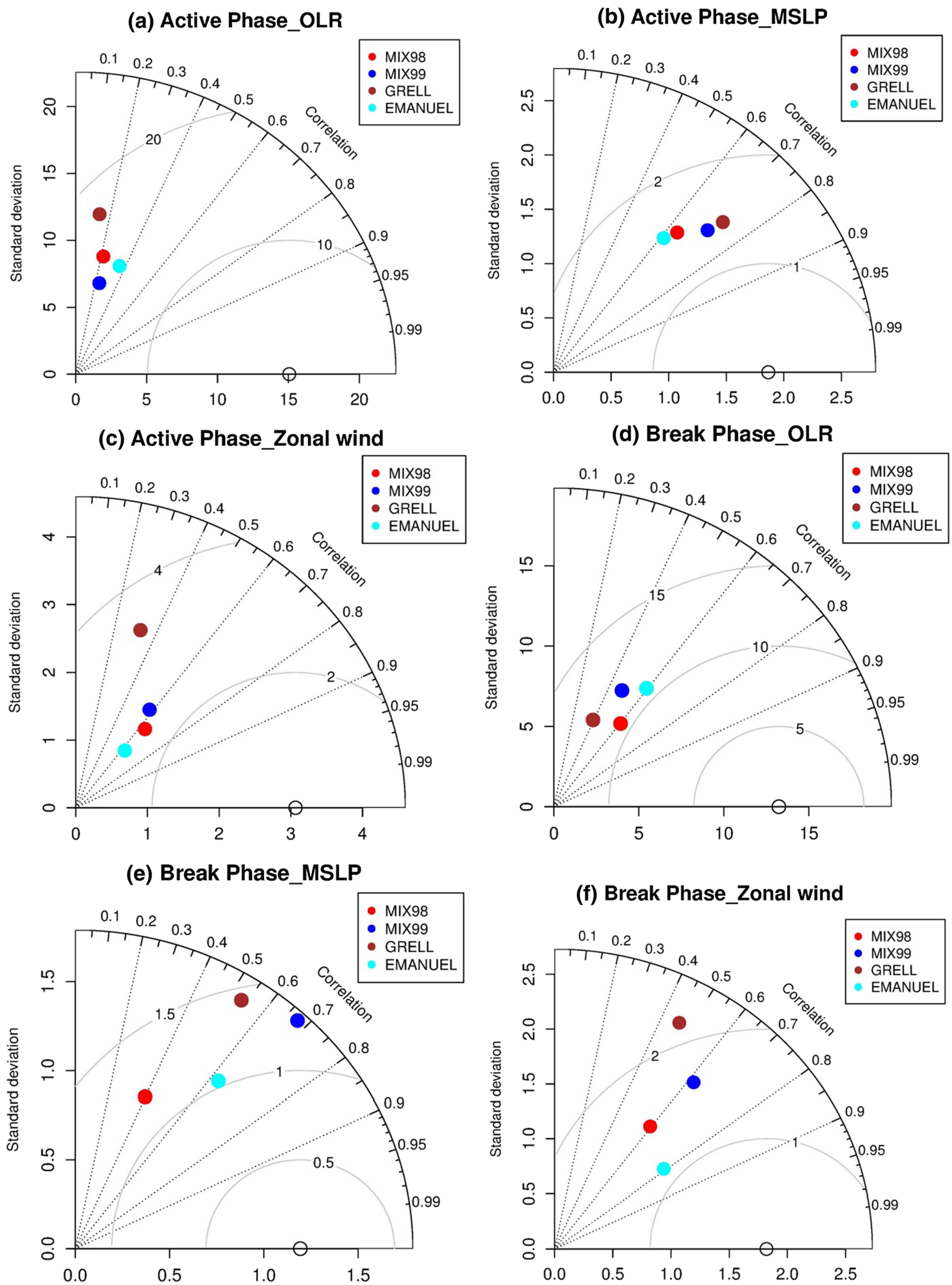

(a) Active Phase_OLR
(b) Active Phase_MSLP
(c) Active Phase_Zonal wind
(d) Break Phase_OLR
(e) Break Phase_MSLP
(f) Break Phase_Zonal wind
MIX98
MIX99
GRELL
EMANUEL
Standard deviation
Correlation
0.1
0.2
0.3
0.4
0.5
0.6
0.7
0.8
0.9
0.95
0.99

performing well over the subcontinent (Mamgain et al. 2013) and Emanuel performs better over ocean (Bhatla and Ghosh 2015). The present study shows the poor performance of Grell CPS over Indian region. But in Mixed scheme mode (Mix99) when the Grell CPS acts over land region and the Emanuel acts over ocean, a satisfactory performance is obtained. The monsoon circulation pattern and statistical scores during the phases are more acceptable in the Mix99 rather than considering the Grell CPS over the whole region. The synoptic features associated with ISM circulation are simulated well for the active as well as break phases with these CPSs. On the other hand, when the Grell scheme acts over ocean region and the Emanuel CPS is applied over the Indian subcontinent, Mix98 could not be able to simulate the phases of monsoon. The considered parameters for this study are basically based on ocean and because of multi-cloud uplift in the Mix99 CPS its convection simulation process is high over the ocean. The updraft mass fluxes of this CPS are represented as a vertical velocity which determines the amount of convective available through potential energy and helps in turn to determine a way to drive the mass fluxes towards the state of quasi-equilibrium for large-scale forcing over the oceanic region. Over subcontinent region, the mechanism is activated with the single cloud uplift process which lifts the parcel by attaining the moist convection over the land subcontinent and is the possible cause behind the success of Mix99 in simulating phases of monsoon. The downdraft mass fluxes are the unique functions of the mass fluxes which are responsible for closeness with the system. Therefore, for the sensitivity study of intra-seasonal monsoon variability using RegCM, use of Mixed scheme (Mix99: Grell over Land and Emanuel over ocean) is the better option for future study.

Acknowledgements

This work is a part of a R&D project, funded by Department of Science and Technology (DST), Govt. of India. The authors wish to thank NOAA/OAR/ESRL (Boulder, Colorado, USA; http://www.esrl.noaa.gov/psd/) and European Centre for Medium-Range Weather Forecasts (ECMWF) for providing gridded datasets. Special thanks to the International Center for Theoretical Physics (ICTP), Italy, for providing the RegCM. The Authors wish to extend their sincere gratitude to the Journal Editor and the Reviewers for their insightful comments on the paper.

References

Achuthavarier, D., Krishnamurthy, V. (2009) Relation between Intra-seasonal and interannual variability of South Asian monsoon in the NCEP forecast system, COLA technical report, pp. 285.

Ajayamohan, R. S., & Goswami, B. N. (2007). Dependence of simulation of boreal summer tropical intra-seasonal oscillations on the simulation of seasonal mean. *Journal of Atmospheric Science, 64*(2), 60–478.

Allan, R. J., & Haylock, M. R. (1993). Circulation features associated with the winter rainfall decrease in southwestern Australia. *Journal of Climate, 6*(7), 1356–1367.

Annamalai, H., & Slingo, J. M. (2001). Active/break cycles: diagnosis of the intra-seasonal variability of the Asian summer monsoon. *Climate Dynamics, 18,* 85–102.

Annamalai, H., Slingo, J. M., et al. (1999). The mean evolution and variability of the Asian summer monsoon: comparison of ECMWF and NCEP-NCAR reanalyses. *Monthly Weather Review Boston MA, 127*(6, Pt. 2), 1157–1186.

Annamalai, H., & Sperber, K. R. (2005). Regional heat sources and the active and break phases of boreal summer intra-seasonal (30–50 days) variability. *Journal of Atmospheric Science, 62,* 2726–2748.

Bhate, J., Unnikrishnan, C. K., & Rajeevan, M. (2012). Regional climate model simulations of the 2009 Indian summer monsoon. *Indian IJRPS, 41*(4), 488–500.

Bhatla, R., & Ghosh, S. (2015). Study of break phase of Indian summer monsoon using different parameterization schemes of RegCM-4.3. *International Journal Of Earth And Atmospheric Science, 2*(3), 109–115.

Bhatla, R., Ghosh, S., Mandal, B., Mall, R. K., & Sharma, K. (2016). Simulation of Indian summer monsoon onset with different parameterization convection schemes of RegCM-4.3. *Atmospheric Research, 176–177,* 10–18.

Bhatla, R., Mohanty, U. C., Raju, P. V. S., & Madan, O. P. (2004). A study on dynamic and thermodynamic aspects of breaks in the summer monsoon over India. *International Journal of Climatology, 24,* 341–360.

Dash, S. K., Pattnayak, K. C., Panda, S. K., Vaddi, D., & Mamgain, A. (2014). Impact of domain size on the simulation of Indian summer monsoon in RegCM4 using mixed convection scheme and driven by HadGEM2. *Climate Dynamics, 44,* 961–975.

Dash, S. K., Shekhar, M. S., & Singh, G. P. (2006). Simulation of Indian summer monsoon circulation and precipitation using RegCM3. *Theoretical and Applied Climatology, 86,* 161–172.

De, U.S., Lele, R.R., & Natu, J.C. (1998) Breaks in southwest monsoon. Pre-Published Scientific Report No. 1998/3.

De, U. S., & Mukhopadhyay, R. K. (2002). Breaks in monsoon and related precursors. *Mausam, 53,* 309–318.

Dickinson, R. E., Errico, R. M., Giorgi, F., & Bates, G. T. (1989). A regional climate model for the Western United States. *Climate Change, 15,* 383–422.

Elguindi, N., Xunqiang, B., Giorgi, F., Nagarajan, B., Pal, J., Solmon, F., Rauscher, S., Zakey, A., & Giuliani, G. (2011) Regional climatic model RegCM user manual version 4.3. The Abdus Salam International Centre for Theoretical Physics, StradaCostiera, Trieste.

Emanuel, K. A. (1991). A scheme for representing cumulus convection in large-scale models. *Journal of Atmospheric Science, 48*(21), 2313–2335.

Emanuel, K. A., & Živković-Rothman, M. (1999). Development and evaluation of a convection scheme for use in climate models. *Journal of Atmospheric Science, 56,* 1766–1782.

Gadgil, S. (2003). The Indian monsoon and its variability. *Annual Review of Earth and Planetary Sciences, 31,* 429–467.

Gadgil, S., Abrol, Y. P., & SeshagiriRao, P. R. (1999). On growth and fluctuation of Indian food grain production. *Current Science, 76,* 548–556.

Gadgil, S., & Joseph, P. V. (2003). On breaks of Indian monsoon. *Proceedings of the Indian Academy of Sciences (Earth and Planetary Sciences), 112,* 529–558.

Ghosh, S., Bhatla, R., Mall, R. K., Srivastava, P. K., & Sahai, Ak. (2018). Aspect of ECMWF downscaled regional climate modeling in simulating Indian summer monsoon rainfall and its dependencies on lateral boundary conditions. *Theoretical and Applied Climatology*. https://doi.org/10.1007/s00704-018-2432-6.

Giorgi, F., & Bates, G. T. (1989). The climatological skill of a regional model over complex terrain. *Monthly Weather Review, 117,* 2325–2347.

Giorgi, F., Coppola, E., Solmon, F., Mariotti, L., Sylla, M. B., Bi, X., et al. (2012). RegCM4: model description and preliminary tests over multiple CORDEX domains. *Climate Research, 52,* 7–29.

Giorgi, F., Diffenbaugh, N. S., Gao, X. J., Coppola, E., Dash, S. K., Frumento, O., et al. (2008). The regional climate change hyper-matrix framework. *Eos, 89*(45), 445–456.

Goswami, B. B., Mukhopadhyay, P., Khairoutdinov, M., & Goswami, B. N. (2012). Simulation of Indian summer monsoon intra-seasonal oscillations in a superparameterized coupled climate model: need to improve the embedded cloud resolving model. *Climate Dynamics, 41,* 1497–1507.

Grell, G. A. (1993). Prognostic evaluation of assumptions used by cumulus parameterizations. *Monthly Weather Review, 121*(3), 764–787.

Holtslag, A. A. M., de Bruijn, E. I. F., & Pan, H. L. (1990). A high resolution air mass transformation model for short-range weather forecasting. *Monthly Weather Review, 118,* 1561–1575.

IPCC. (2007). Climate Change 2007. The physical science basis. Contribution of Working Group I to the Fourth Assessment Report of the Intergovernmental Panel on Climate Change. In S. Solomon, D. Qin, M. Manning, Z. Chen, M. Marquis, K. B. Averyt, M. Tignor, H. L. Miller (Eds.) (p. 996). Cambridge, UK: Cambridge University Press.

Kang, H. S., & Hong, S. Y. (2008). Sensitivity of the simulated East Asian summer monsoon climatology to four convective parameterization schemes. *Journal of Geophysical Research Atmospheres, 113,* 1–17.

Krishna Kumar, K., Rupa Kumar, K., Ashrit, R. G., Deshpande, N. R., & Hansen, J. W. (2004). Climate impacts on Indian Agriculture. *International Journal of Climatology, 24,* 1375–1393.

Krishnamurti, T. N., & Ardanuy, P. (1980). The 10 to 20-day westward propagating mode and ''breaks in the monsoons''. *Tellus, 32,* 15–26.

Krishnan, R., Zhang, C., & Sugi, M. (2000). Dynamics of breaks in the Indian summer monsoon. *Journal of Atmospheric Science, 57,* 1354–1372.

Lal, M., Meehl, G. A., & Arblaster, J. M. (2000). Simulation of Indian summer monsoon rainfall and its intra-seasonal variability in the NCAR climate system model. *Regional Environmental Change, 1,* 163–179.

Lau, K. M., & Chan, P. H. (1986). Aspects of the 40–50 day oscillation during the northern summer as inferred from outgoing longwave radiation. *Monthly Weather Review, 114,* 1354–1367.

Lawrence, D. M., & Webster, P. J. (2002). The boreal summer intra-seasonal oscillation: relationship between northward and eastward movement of convection. *Journal of Atmospheric Science, 59,* 1593–1606.

Li, F., Chambers, L. E., & Nicholls, N. (2005). Relationships between rainfall in the southwest of Western Australia and near-global patterns of sea-surface temperature and mean sea-level. *Australian Meteorological Magazine, 54,* 23–33.

Maharana, P., & Dimri, A. P. (2015). Study of intra-seasonal variability of Indian summer monsoon using a regional climate model. *Climate Dynamics, 46,* 1043. https://doi.org/10.1007/s00382-015-2631-0.

Mamgain, A., Mariotti, L., Coppola, E., Giorgi, F., & Dash, S. K. (2013). Sensitivity of RegCM4.3 two convection schemes on Indian summer monsoon for the South Asia CORDEX domain. *EGU General Assembly Conference Abstracts, 15,* 4812.

National Climate Centre (NCC) Research Report. (2013) Development and analysis of a new high spatial resolution (0.25° × 0.25°) long period (1901–2010) daily gridded rainfall data set over India. In D. S. Pai, Latha Sridhar, M. Rajeevan, O. P. Sreejith, N. S. Satbhai, B. Mukhopadhyay (Eds.) (p. 63). NCC Research Report No. 1/2013.

ParthSarthi, P., Ghosh, S., & Kumar, P. (2015). Possible Future Projection of Indian Summer Monsoon Rainfall (ISMR) with the evaluation of model performance in Coupled Model Inter-comparison Project Phase 5 (CMIP5). *Global and Planetary Change, 129,* 92–106.

ParthSarthi, P., Kumar, P., & Ghosh, S. (2016). Possible future rainfall over the gangetic plains (GP), India, in multi model simulations of CMIP3 and CMIP5. *Theoretical and Applied Climatology, 124*(3–4), 691–701. https://doi.org/10.1007/s00704-015-1447-5.

Rajeevan, M., Gadgil, S., & Bhate, J. (2010). Active and break spells of the Indian summer monsoon. *Journal of Earth System Science, 119*(3), 229–247.

Raju, P. V. S., Bhatla, R., Almazroui, M., & Assiri, M. (2015). Performance of convection schemes on the simulation of summer monsoon features over the South Asia CORDEX domain using RegCM-4.3. *International Journal of Climatology, 35*(15), 4695–4706. https://doi.org/10.1002/joc.4317.

Raju, P. V. S., Bhatla, R., & Mohanty, U. C. (2009). The evolution of mean conditions of surface meteorological fields during active/break phases of the Indian summer monsoon. *Theoretical and Applied Climatology, 95,* 135–149.

Ramamurthy, K. (1969) Monsoon of India: Some aspects of the 'break' in the Indian southwest monsoon during July and August. In *Forecasting Manual 1–57 No. IV 18.3*. Pune, India: India Meteorological Department.

Rao, Y. P. (1976). Southwest monsoon India Meteorological Department. *Meteorological Monograph Synoptic Meteorol, 1*, 367.

Reynolds, R. W., Rayner, N. A., Smith, T. M., Stokes, D. C., & Wang, W. (2002). An improved in situ and satellite SST analysis for climate. *Journal of Climate, 15,* 1609–1625.

Sardar, S., Ahmad, I., ShoaibRaza, S., & Irfan, N. (2012). Simulation of south Asian physical environment using various cumulus parameterization schemes of MM5. *Meteorological Applications, 19,* 140–151.

Sikka, D. R., & Gadgil, S. (1980). On the maximum cloud zone and the ITCZ over Indian longitudes during the southwest monsoon. *Monthly Weather Review, 108,* 1840–1853.

Singh, D., Tsiang, M., Rajaratnam, B., & Diffenbaugh, N. S. (2014). Observed changes in extreme wet and dry spells during the South Asian summer monsoon season. *Nature Climate Change, 4,* 456–461. https://doi.org/10.1038/nclimate2208.

Sinha, P., Mohanty, U. C., Kar, S. C., Dash, S. K., & Kumari, S. (2013). Sensitivity of the GCM driven summer monsoon simulations to cumulus parameterization schemes in nested RegCM3. *Theoretical and Applied Climatology, 112,* 285–306. https://doi.org/10.1007/s0070401207285.

Taraphdar, S., Mukhopadhyay, P., & Goswami, B. N. (2010). Predictability of Indian summer monsoon weather during active and break phases using a high resolution regional model. *Geophysical Research Letters, 37,* L21812.

Taylor, K. E. (2001). Summarizing multiple aspects of model performance in a single diagram. *Journal of Geophysical Research, 106*(D7), 7183–7192.

Umakanth, U., Kesarkar, A. P., Raju, A., & VijayaBhaskarRao, S. (2015). Representation of monsoon intra-seasonal oscillations in regional climate model: sensitivity to convective physics. *Climate Dynamics, 47*(3–4), 895–917. https://doi.org/10.1007/s00382-015-2878-5.

Varikoden, H. (2006) Dynamic characteristics of atmospheric boundary layer during different phases of monsoon. Doctoral Thesis. Department of Atmospheric Sciences Cochin University of Science and Technology, Lakeside Campus, Cochin, India.

Wang, B., & Rui, H. (1990). Synoptic climatology of transient tropical intra-seasonal convection anomalies: 1975–1985. *Meteorology and Atmospheric Physics, 44,* 43–61.

Wilk, M. B., & Gnanadesikan, R. (1968). Probability plotting methods for the analysis of data. *Biometrika, 55*(1), 1–17.

(Received December 12, 2017, revised March 22, 2018, accepted April 30, 2018, Published online May 10, 2018)